Nikolić, S., Opsenica, D. M., Filipović, V., Dojčinović, B. P., Aranđelović, S., Radulović, S.,& Grgurić-Šipka, S.. (2015). Strong in Vitro Cytotoxic Potential of New Ruthenium-Cymene Complexes. in Organometallics

Amer Chemical Soc, Washington., 34(14), 3464-3473.

https://doi.org/10.1021/acs.organomet.5b00041

Strong *in vitro* Cytotoxic Potential of New Ruthenium-Cymene Complexes

Stefan Nikolić[†], Dejan M. Opsenica[‡]*, Vuk Filipović[‡], Biljana Dojčinović[‡], Sandra Aranđelović[§], Siniša Radulović[§], Sanja Grgurić-Šipka[†]*

[†]*Faculty of Chemistry, University of Belgrade, Studentski trg 12-16, 11000 Belgrade, Serbia*

[‡]*Institute of Chemistry, Technology and Metallurgy, University of Belgrade, Njegoševa 12, 11000, Belgrade, Serbia*

[§]*Institute for Oncology and Radiology of Serbia, Pasterova 14, 11000 Belgrade, Serbia*

Graphic for Table of Contents and Abstract

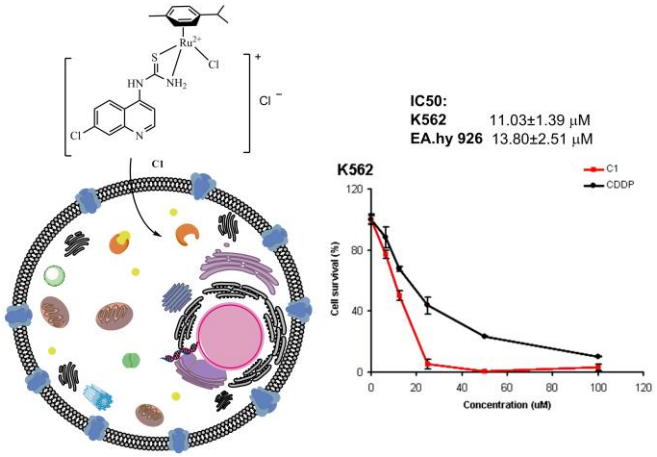

ABSTRACT: Two *p*-cymeneruthenium chlorido complexes with thiourea derivative of 7-chloroquinoline (**C1**) and pyridine-3-imidazole (**C2**) were synthesized starting from $[(\eta^6\text{-}p\text{-cymene})RuCl_2]_2$ and corresponding ligands. The structures of complexes were determined with elemental analysis, IR, ESI-MS, ^1H, $^{13}C\{^1H\}$ NMR and 2D ^1H-^{15}N correlation NMR spectroscopy. Cytotoxic activities examined by MTT assay were performed in five human neoplastic cell lines (HeLa, K562, A549, MDA-MB-231, EA.hy926) and one non-tumor human fetal lung fibroblast cell line (MRC-5). Tested complexes exhibited low micro-molar activities with IC_{50} in the range 11.03 - 56.45μM, while ligands **L1**, **L2** were significantly less active. Complex **C1** showed cytoselective activity toward K562 cell-line (IC_{50}=11.03±1.39 μM), and was three times less active against non-tumor MRC-5 cell line. Flow cytometry analysis indicated that complexes **C1** and **C2** after 24 hours treatment, caused concentration dependent increase of apoptotic Sub-G1 fraction (up to 18.4%), comparable to *cis*-diamminedichloridoplatinum(II) (cisplatin, **CDDP**), though without other substantial alterations of cell cycle. Drug-accumulation and DNA-binding study performed by ICP-MS in K562 cell-line revealed that complex **C1** had high intracellular uptake (1.38 μgRu/10^6 cells), which significantly exceeded the intracellular uptake levels of **CDDP (**0.29 μgPt/10^6 cells) and **C2 (**0.08 μgRu/10^6 cells) intracellular uptakes. However, both ruthenium complexes, **C1** and **C2**, bind to cellular DNA less efficiently in comparison to **CDDP**. Structure-activity relationship clearly suggested that introduction of 7-chloroquinoline moiety in ruthenium(II)-*p*-cymene complex significantly contributed to the intracellular uptake of **C1**, and higher cytotoxicity and cytoselectivity.

INTRODUCTION

During the last decades, ruthenium arene complexes were attracted significant attention, due to their advanced chemical and air stability, water solubility and structural diversity finally promoted them as highly potent anticancer agents.[1] The arene ligands are strongly bonded to the ruthenium center and are relatively inert towards substitution reactions stabilizing the metal ion in lower oxidation state. In addition, such complexes have somewhat higher hydrophobicity which is necessary for the passive transport across cell membranes. The three remaining ruthenium coordination sites can be occupied with other ligands, forming the "piano stool" geometry, typical for organoruthenium(II) complexes.[2,3] Organoruthenium complexes which contains a π-bonded arene and various of mono- or bidentate ligands are considered as promising candidates for treatment of cancer.[4]

Synthesis of complexes containing bioactive compounds as ligands directly coordinated to transition metal ions with the aim to obtain compounds with improved biological activities seems to be a promising strategy.[5] A great number of quinoline-based metal complexes were synthesized since it was discovered that they exhibit diverse pharmacological properties, such as antifungal, antitumor or antiviral activity.[6] In addition, synthetic quinoline-based drugs like, chloroquine and primaquine are still the most important drugs in malaria treatment.[7,8]

Introducing the bioactive compounds as ligands was successfully applied to the ruthenium arene complexes with chloroquine analogues.[9] Combination of the ruthenium arene moiety with different chloroquine derivatives lead to complexes that demonstrated significant *in vitro* cytotoxicity with apoptosis as mechanism of cell death.[10,11] Recent studies on ruthenium complexes with the quinolone showed an increased toxicity against selected cancer cell lines.[12,13]

Synthesis of two new ruthenium(II)-cymene complexes has been reported here along with their cytotoxic activities against five human neoplastic cell lines. One complex was prepared with a new ligand, 1-(7-chloroquinolin-4-yl)thiourea **L1**, and the other with 3-(4,5-dihydro-1*H*-imidazol-2-yl)pyridine hydrochloride **L2**. Ligands **L1** and **L2** significantly differs in structures and modes of coordination. **L1** is quinoline based ligand. From literature it is well established that mechanism of action of wide spectrum of biologically active compounds derived from quinoline, are based on π-staking interactions with protoporphyrine IX (malaria)[14] or DNA/RNA (cancer).[15] Ligand **L1** was designed to be coordinated to central ion *via* thioamide group, and leave quinoline core available for interactions with target. Contrary to that, **L2** was chosen to achieve coordination *via* pyridine moiety. To our best knowledge, ligands **L1** and **L2** were never before used as ligands for synthesis of biologically active transition metal complexes. Ligand **L1** is new compound and this study is very first examination of its cytotoxic activity. Ligand **L2** is known from literature, but informations about its biological activities are meagre. In recently published article the capabilities for binding to imidazoline sites (I_1 and I_2) and α–adrenergic receptors (α_1 and α_2) was examined.[16] The results obtained in this study reveal strong anticancer activity of the synthesized complexes, even against A549 cell line which is considered to be only moderately sensitive to cisplatin.[17]

EXPERIMENTAL SECTION

Material and methods. $RuCl_3 \times 3H_2O$ was purchased from Johnson Matthey (London, United Kingdom). $[(\eta^6\text{-}p\text{-cymene})RuCl_2]_2$ was prepared according to a published procedure.[18] Solvents and other reagents were purchased from various suppliers and were used without additional purification. Elemental analysis was carried out with Elemental Vario EL III microanalyzer.

Infrared spectra were recorded on a Nicolet 6700 FT-IR spectrometer using ATR or KBr pellet technique. ^{1}H and $^{13}C\{^{1}H\}$ NMR spectra were recorded on a Varian Gemini-200 spectrometer (at 200 and 50 MHz, respectively) and on a Bruker Ultrashield Advance III spectrometer (at 500 and 125 MHz, respectively) employing indicated solvents (vide infra) using TMS as the internal standard. Chemical shifts are expressed in ppm (δ) values and coupling constants (J) in Hz.

ESI mass spectra of ligands were recorded on 6210 Time-of-Flight LC-MS instrument (G1969A, Agilent Technologies) in positive ion mode with CH_3CN/H_2O. ESI mass spectra measurements of complexes were carried out on a MS system LTQ Orbitrap XL with heated ESI ionization in methanol solutions. Electronic spectra of solutions of complexes were recorded in acetonitrile, using a GBC UV/ Vis Cintra 6 spectrophotometer. Melting points were determined on an Electrothermal melting point apparatus. Conductivity measurements were done using a Crison Multimeter MM 41 instrument. Conductivities of complexes were carried out with 1 mM solutions in acetonitrile, DMSO and methanol. Reactions carried out employing microwave (MW) conditions were performed using a Biotage Initiator Eight Robot with an automatic sampler (USA and Sweden).

Synthesis

7-chloro-4-isothiocyanatoquinoline (**2**).[19] A mixture of 4,7-dichloroquinoline (**1)** (500 mg, 2.52 mmol) and silver-thiocyanate (830 mg, 5.0 mmol) in anhydrous toluene (4 mL) was heated 18 hours (oil bath, 115 °C). The hot reaction mixture was filtered and washed three times with DCM (3×10 mL). The combined filtrates were concentrated under reduced pressure to afford the 7-chloro-4-isothiocyanatoquinolineas as yellow solid. Yield: 490 mg (89%).^{1}H NMR (500 MHz,

CD_3OD): δ_H 8.81 (1H, d, J = 5.1 Hz, H2), 8.07 (1H, d, J = 9.1 Hz, H5), 8.00 (1H, d, J = 2.05 Hz, H8), 7.90 (1H, d, J = 5.0 Hz, H3), 7.59 (1H, dd, J_1 = 2.05, J_2 = 9.1, Hz, H6).

1-(7-chloroquinolin-4-yl)thiourea (L1). 7-chloro-4-isothiocyanatoquinoline (**2**) (450 mg, 2.05 mmol) was dissolved in MeOH/NH_3 (methanol saturated with NH_3 gas, 10 mL) and the mixture was stirred for 2 days at room temperature. The solvent was evaporated, solid was dissolved in DCM and washed once with water, once with brine and dried over anhydrous Na_2SO_4. Solvent was removed under reduced pressure and residue was purified through silica-gel dry-flash column using DCM/MeOH(NH_3) (9/1) as eluent. Yield: 308 mg (59%). Mp = 220 ^oC decomp. Anal. Calcd. for ($C_{10}H_8ClN_3S\times H_2O$): calculated C 46.97, H 3.94, N 16.43, S 12.54; found C 47.54, H 4.24, N 16.11, S 12.24.[20] IR(ATR): 3268 (s), 3124 (s), 2962 (s), 1735 (m), 1641 (s), 1610 (s), 1592 (m), 1568 (m), 1491 (s), 1448 (m), 1421 (s), 1374 (m), 1352 (m), 1312 (m), 1251 (s), 1192 (w), 1161 (w), 1111 (m), 1075 (w), 1055 (m), 908 (w), 876 (m), 828 (m), 803 (w), 768 (w), 732 (w), 634 (w), 616 (w), 585 (w). ^1H NMR (500 MHz, DMSO-d_6): δ_H 9.97 (1H, br s, Ar-NH), 8.83 (1H, d, $^3J_{(H2, H3)}$ = 4.8Hz, H2), 8.33 (1H, br s, S=C-NH_2), 8.11 (1H, d, $^3J_{(H5, H6)}$ = 9.0 Hz, H5), 8.05 (1H, d, $^4J_{(H6, H8)}$ = 2.0 Hz, H8), 8.01 (1H, d, $^3J_{(H2, H3)}$ = 5.0Hz, H3), 7.68 (2H, m, H6 and S=C-NH_2). $^{13}C\{^1H\}$ NMR (125 MHz, DMSO-d_6): δ_C 182.21 (C9), 151.79 (C2), 149.13 (C8a), 143.24 (C4), 134.19 (C7), 127.80 (C8), 126.66 (C6), 124.74 (C5), 121.59 (C4a), 115.69 (C3). (+)ESI-MS (m/z): $[M+H]^+$ Calculated 238.02002, found 238.01970.

2-pyridine-3-yl-4,5-dihydro-1H-imidazole hydrochloride (L2×HCl). A mixture of 3-cyanopyridine **3** (250 mg, 2.40 mmol), ethylenediamine (3.0 mL, 44.92 mmol) and sulphur (154 mg, 4.8 mmol) was heated in a MW reactor (110 °C) for 1.5 hour. Reaction mixture was cooled to room temperature and evaporated to dryness. Residue was dissolved in dichloromethane (30 mL), washed once with water (10 mL), once with brine (15 mL) and the organic layer was dried

over anhydrous Na_2SO_4. Solvent was removed under reduced pressure, residue was dissolved in MeOH/HCl (MeOH saturated with HCl gas, 30 mL) and stirred at r.t. for 2 hours. Mixture was evaporated to dryness, and HCl salt was triturated in dry MeOH (5 mL). Product was filtered and dried under reduced pressure in the vacuum oven. 2-pyridine-3-il-4,5-dihydro-1H-imidazole hydrochloric salt is a pale yellow solid. Yield: 220 mg (51%). Mp 248 - 250 ^{o}C. IR (ATR): 3503 (w), 2915 (s), 2804 (s), 2713 (s), 2678 (s), 2575 (m), 2519 (m), 2443 (m), 2054 (m), 1603 (m), 1555 (w), 1507 (s), 1343 (w), 1085 (w), 1033 (m), 1008 (w), 819 (w), 685 (w) cm^{-1}. ^{1}H NMR (200 MHz, DMSO-d_6): δ_H 11.46 (2H, 2×NH, br s), 9.39 (1H, bs, H2), 8.95 (1H, d, $^{3}J_{(H5, H6)}$ = 4.5Hz, H6), 8.74 (1H, dt, $^{3}J_{(H4, H5)}$ = 8.3, $^{4}J_{(H4, H2)}$ = 1.8, H4), 7.81 (1H, dd, $^{3}J_{(H4, H5)}$ = 8.1, $^{3}J_{(H5, H6)}$ = 4.8, H5), 4.01 (4H, s, H8 and H9). ^{13}C{^{1}H} NMR (50 MHz, DMSO-d_6): δ_C 162.88 (C7), 153.31 (C6), 148.39 (C2), 138.47 (C4), 124.91 (C5), 119.86 (C3), 44.69 (C8 and C9).

[(η^6-p-cymene)Ru(L1)Cl]Cl (C1). To a warm solution (35 °C) of **L1** (63 mg, 0.262 mmol) in CH_2Cl_2/MeOH mixture (40 mL, V/V = 3/1), [Ru(η^6-*p*-cymene)Cl_2]$_2$ (80 mg, 0.131 mmol) in CH_2Cl_2 (2 mL) was added in one portion. The color of the reaction mixture has changed from orange to dark red. The reaction mixture was cooled to room temperature, stirred for 20 h and placed in a fridge for two days. The red powder was filtered off, washed with hexane and dried *in vacuum*. Yield: 86 mg (58%). Anal. Calcd. for $C_{20}H_{22}Cl_3N_3RuS$: C, 44.16; H, 4.08; N, 7.73. Found: C, 43.77; H, 4.53; N, 7.39. IR (ATR, cm^{-1}): 3277.4 (s), 3073.8 (s), 2995.9 (w), 2957.5 (w), 2870.5 (w), 2701.9 (s), 2645.7 (m), 1624.6 (s), 1586.2 (m), 1471.9 (s), 1414.4 (m), 1366.2 (s), 1344.8 (s), 1238.6 (w), 1208.3 (m), 832.0 (w), 644.2 (w). ^{1}H NMR (500 MHz, DMSO-d_6): δ_H 8.88 (1H, d, $^{3}J_{(H2, H3)}$ = 5.4 Hz, H2), 8.59 (1H, bs S=C-NH_2), 8.37-8.32 (2H, m, H3 and H5), 8.16 (1H, bs S=C-NH_2), 8.10 (1H, d, $^{4}J_{(H6, H8)}$ = 2.1 Hz, H8), 7.76 (1H, dd, $^{3}J_{(H5, H6)}$ = 9.1, $^{4}J_{(H6, H8)}$ = 2.2 Hz, H6), 5.84 – 5.75 (4H, m, H11, H11", H12 and H12'), 2.88-2.78 (1H, m, H15), 2.09

(3H, s, H14), 1.19 (6H, d, $^{3}J_{(H15,\ H16)}$ =7.0 Hz H16 and H16'). $^{13}C\{^{1}H\}$ NMR (125 MHz, DMSO-d_6): δ_C 182.03 (C9), 149.38 (C2), 145.96 (C8a and C4), 135.56 (C7), 127.20 (C6), 125.21 (C8 and C5), 120.50 (C4a), 113.31 (C3), 106.35 (C13), 100.06 (C10), 86.34 (C12 and C12'), 85.48 (C11 and C11'), 29.94 (C15), 21.47 (C16 and C16'), 17.84 (C14). (+)ESI-MS (*m*/*z*): [(η^6-*p*-cymene)Ru(L1-H)]$^+$ Calculated 472.01776, found 472.0189.

[(η^6-p-cymene)Ru(HL2)Cl$_2$]BPh$_4$ (C2). To a solution of **L2×HCl** (36 mg, 0.196 mmol) in ethanol (6 mL), [Ru(η^6-*p*-cymene)Cl$_2$]$_2$ (60 mg, 0.098 mmol) in ethanol (4 mL) was added in one portion. The color of the reaction mixture has changed from red to dark orange. The reaction mixture was stirred at room temperature for 48 h. Sodium-tetraphenylborate (67 mg, 0.196 mmol) was added, and the resulting yellow precipitate was filtered off, washed with diethyl-ether and dried *in vacuo*. Yield: 105 mg (68%). Anal. Calcd. for $C_{42}H_{44}Cl_2N_3Ru$: C, 65.49; H, 6.01; N, 5.33. Found: C, 64.86; H, 6.01; N, 5.44.[20] IR (ATR, cm^{-1}): 3300.0 (s), 3117.2 (m), 3055.7 (s), 2965.8 (m), 1621.7 (s), 1580.2 (w), 1475.9 (m), 1426.0 (m), 1379.5 (w), 1291.2 (m), 1032.9 (w), 737.0 (s), 707.0 (s), 612.8 (m). ^{1}H NMR (200 MHz, DMSO-d_6): δ_H 10.70 (2H, 2×NH, br s), 9.09 (1H, d, $^{3}J_{(H2,\ H4)}$ = 2.2, H2), 8.90 (1H, dd, $^{3}J_{(H5,\ H6)}$ = 4.8, $^{4}J_{(H4,\ H6)}$ = 1.4 Hz, H6), 8.29 (1H, dt, $^{3}J_{(H4,\ H5)}$ = 7.9, $^{3}J_{(H2,\ H4)}$ = 2.0, H4), 7.68 (1H, dd, $^{3}J_{(H4,\ H5)}$ = 8.1, $^{3}J_{(H5,\ H6)}$ = 4.8Hz, H5), 7.20 (8H, br s, H2-BPh$_4$), 7.00-6.86 (8H, m, H3-BPh$_4$), 6.85-6.72 (4H, m, H4-BPh$_4$), 5.83-5.73 (4H, m, H11, H11'', H12 and H12'), 4.03 (4H, s, H8 and H9), 2.95-2.77 (1H, m, H15), 2.12 (3H, s, H14), 1.22 (6H, d, $^{3}J_{(H15,\ H16)}$ = 6.7 Hz, H16 and H16'). $^{13}C\{^{1}H\}$ NMR (50 MHz, DMSO-d_6) δ_C 163.90 (C7), 163.61 (C1-BPh$_4$), 155.04 (C6), 149.19 (C2), 136.41 (C4), 135.79 (C2-BPh$_4$), 125.55 (C3-BPh$_4$), 124.38 (**C**5), 121.77 (C4-BPh$_4$), 119.23 (**C**3), 106.61 (C13), 100.33 (C10), 86.60 (C12 and C12'), 85.74 (C11 and C11'), 44.80 (C8 and C9), 30.18 (C15), 21.69 (C16 and C16'),

18.07(C14). (+)ESI-MS (*m*/*z*): $[(\eta^6\text{-}p\text{-cymene})Ru(L2\text{-}H)]^+$ Calculated 382.084664, found 382.0903.

Bioassays. For biological examination (intracellular accumulation, interactions with DNA, cytotoxicity) the complexes **C1**, **C2** and corresponding ligands **L1**, **L2×HCL** were dissolved in DMSO (10 mM), prior to use. DMSO solutions were mixed with the aqueous solutions used in biological studies immediately prior to use, so that final concentration of DMSO never exceeded 0.1% (v/v).

Reagents and cell cultures. Five human tumor cell lines: human cervix adenocarcinoma (HeLa), human myelogenous leukemia (K562), human alveolar basal adenocarcinoma (A549), human breast adenocarcinoma (MDA-MB-231), human umbilical vein endothelial cells (EA.hy 926) and one non-tumor human lung fibroblast cell line (MRC-5) were maintained as monolayer culture in nutrient medium, Dulbecco`s Modified Eagle Medium (DMEM). Powdered DMEM medium was purchased from Sigma-Aldrich Co. Nutrient mediums were prepared in sterile deionized water, supplemented with penicillin (192 U/mL), streptomycin (200 μg/mL), 4-(2-hydroxyethyl)piperazine-1-ethanesulfonic acid (HEPES) (25 mM), L-glutamine (3 mM), 10% of heat-inactivated fetal calf serum (FCS) (pH 7.2). For maintaining the EA.hy 926 cells, DMEM was additionally supplemented with D-Glucose (4.5 g/L). The cells were grown at 37 °C in 5% CO_2 and humidified at air atmosphere.

MTT assay. Cytotoxicity of tested complexes was determined by using 3-(4,5-dimethylthiazol-yl)-2,5-diphenyltetrazolium bromide (MTT, Sigma-Aldrich) assay.[21,22] Cells were seeded into 96-well cell culture plates (Thermo Scientific Nunc™), at a cell density of: 4000 c/w (HeLa); 8000 c/w (A549); 7000 c/w (MDA-MD-231 and MRC-5); 3000 c/w (EA.hy 926); and 5000 c/w (K562), in 100 μL of culture medium. After 24 hours of growth, cells were exposed to the serial

dilutions of the tested complexes. Serial dilutions were made in culture medium, so that final concentrations achieved per wells were 6.25 μM, 12.5 μM, 25 μM, 50 μM and 100 μM. Each concentration was tested in triplicates. After incubation periods of 72 hours, 20 μL of MTT solution, 5 mg/mL in phosphate buffer solution, pH 7.2 were added to each well. Samples were incubated for 4 hours at 37 °C, with 5% CO_2 in humidified atmosphere. Formazan crystals were dissolved in 100 μL of 10% sodium dodecyl sulfate (SDS). Absorbances were recorded after 24 hours, on an enzyme-linked immunosorbent assay (ELISA) reader (ThermoLabsystems Multiskan EX 200–240 V), at the wavelength of 570 nm. IC_{50} values (μM) were determined from the cell survival diagrams. The percentages of surviving cells relative to untreated controls were determined. The IC_{50} value, defined as the concentrations of the compound causing 50% cell growth inhibition, was estimated from the dose-response curves.

Flow-cytometric analysis of cell cycle phase distribution. Quantitative analysis of cell cycle phase distribution was performed by flow-cytometric analysis of the DNA content in fixed K562 cells, after staining with propidium iodide (PI).[23] Cells were seeded at density of 3×10^5 cells per well, into 6-well plates (Thermo Scientific Nunc™), in 2 mL of nutrition medium. After 24 hours of growth, cells were exposed to the investigated complexes, ligands or *cis*-diamminedichloridoplatinum(II) (cisplatin, **CDDP**) at concentrations corresponding to the IC_{50} or $2 \times IC_{50}$ values. After 24 hours of continuous treatment cells were collected, washed twice with ice-cold PBS, and fixed overnight in 70% ethanol. After fixation cells were washed with PBS, and incubated with RNaseA (1 mg/mL) for 30 min at 37 °C. Immediately before flow-cytometric analysis, cells were stained with PI, at concentration of 400 mg/mL. Cell cycle phase distribution was analyzed using a fluorescence activated sorting cells (FASC) Calibur Becton Dickinson flow cytometer and Cell Quest computer software.

Microwave digestion. The digestion was performed on Advanced Microwave Digestion System (ETHOS 1, Milestone, Italy) using HPR-1000/10S high pressure segmented rotor. The pressure-resistant PTFE vessels used in this study were consisted of the fluoropolymer liner. Before use, the PTFE vessels were acid cleaned and rinsed with deionized water. This type of vessel endures maximum temperature of 240 ºC and a maximum pressure of 100 bar. A maximum of 10 PTFE vessels could simultaneously be mounted on the rotor. The internal temperature was monitored with one vessel equipped with a sensor unit only, and this vessel had a sensor-protecting tube that was in direct contact with the digested solution, differing from the other common PTFE vessels. The entire sample was precisely and quantitatively transferred and mixed in each clean vessel with 7 mL HNO_3 (65%) and 1 mL H_2O_2 (30%) (Suprapure®, Merck, Germany) and then microwave heated for 10 min. The temperature was controlled by using a predetermined power program. The temperature was typically raised to 200 ºC in the first 10 min, and to a peak temperature of 200 ºC in the next 10 min, and then cooled down rapidly. After cooling and without filtration, the solution was diluted to a fixed volume into a 10 mL volumetric flask and made up to volume with ultra-pure water. Ultra-pure water resistivity of 18.2 MΩ/cm was prepared using a Milli-Q system (Millipore, Bedford, MA, USA).

Measurement of intracellular ruthenium(II) accumulation using ICP-MS. Ruthenium accumulation was analyzed in K562 cells, using inductively coupled plasma mass spectrometry (ICP-MS). K562 cells were seeded at density of 7×10^5, into 25 cm^2 dishes (Thermo Scientific Nunc™). At the exponential phase of growth, cells were treated with the investigated complexes (**C1** and **C2**) or **CDDP** at equimolar concentration of 50 μM. After 24 hours, cells were collected by centrifugation at 1000 rpm, 10 min. Cell pellet was washed by ice cold PBS and cell viability was determined by tripan-blue exclusion test. Measurement of ruthenium(II) content in HeLa

cells, was analyzed, by using ICP-MS and Thermo Scientific iCAP Qc ICP-MS (Thermo Scientific, Bremen, Germany) spectrometer with operational software Qtegra. The instrument was optimized for optimum performance in He KED (Kinetic Energy Discrimination) mode using the supplied autotune protocols. Standards for the instrument calibration were prepared on the basis of ruthenium, plasma standard solution, Specpure®, Ru 1000µg/mL certified reference solution ICP Standard purchased from Alfa Aesar GmbH & Co KG (Germany).[24]

Measurement of ruthenium(II)-DNA-binding using ICP-MS. Binding of ruthenium to cellular DNA was analyzed in K562 cells, by using ICP-MS. K562 cells were seeded at density of 2×10^6, into 75 cm^2 dishes (ThermoScientificNunc™) and at the exponential growth phase cells, were treated with the tested complexes or **CDDP** at equimolar concentration of 50 µM. After 24 hours treatment, cells were collected, washed by ice cold PBS and cell pellet was collected by centrifugation at 1000 rpm, for 10 min. Cell number was determined by tripan-blue exclusion test. Total DNA was isolated by using salting out procedure, as previously described,[25,26] and concentrations were determined spectrophotometrically by measuring absorbance at A260/A280nm, at BioSpec-nano (Shimadzu Biotech).

RESULTS AND DISCUSSION

Synthesis of ligands. Ligand **L1** is a new compound and it was synthesized from isothiocyanate derivative **2** (Scheme 1). Starting from 4,7-dichloroquinoline **1**, using silver-isothiocyanate in anhydrous toluene after 18 hours 4-isothiocyanate derivative **2** was obtained.[27] Stirring of solution of **2** in methanol saturated with gaseous ammonia at room temperature during 2 days, isocyanate was transformed in to corresponding 4-thiourea **L1**.

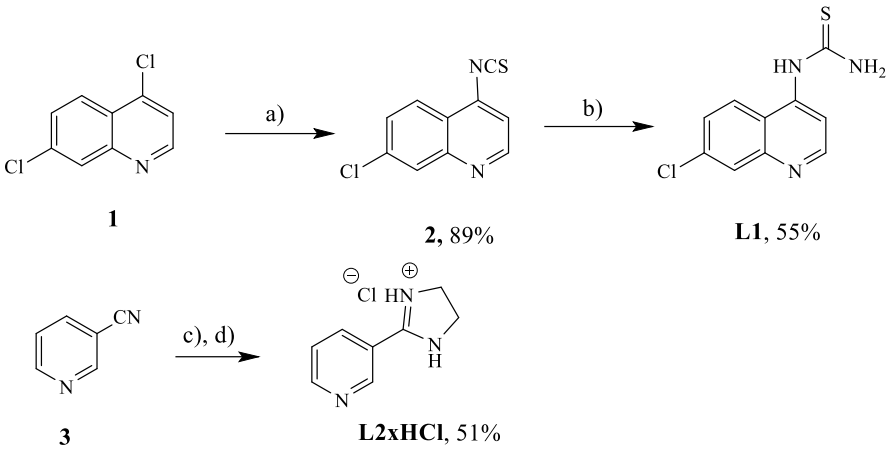

a) AgSCN, PhMe, 115°C; b) MeOH / NH_3, r.t.; c) ethylendiamine, S, MW; d) MeOH / HCl

Scheme 1. Synthetic route to ligands **L1** and **L2×HCl**

Ligand **L2×HCl** is a known compound and many different procedures for its synthesis starting from corresponding 3-cyanopyridine were described.[28] Procedure with sulphur as reducing agent was applied here, by using MW instead ultra-sound (Scheme 1).[29]

Synthesis of complexes. Complexes **C1** and **C2** were obtained from $[(\eta^6\text{-}p\text{-cymene})RuCl_2]_2$ dimer and ligands **L1** or **L2×HCl** respectively, in 1:2 molar ratio (Scheme 2). Applying this method, in CH_2Cl_2/MeOH mixture, at 35°C, red complex **C1** was obtained in good yield (58%). The complex **C1** is soluble in DMSO, DMF, and methanol and partially soluble in water. The complex **C2** was obtained in ethanol as solvent, at room temperature using the method described above, with **L2×HCl** in good yield (68%) as a yellow solid. The complex **C2** has good solubility in DMSO, DMF and acetonitrile.

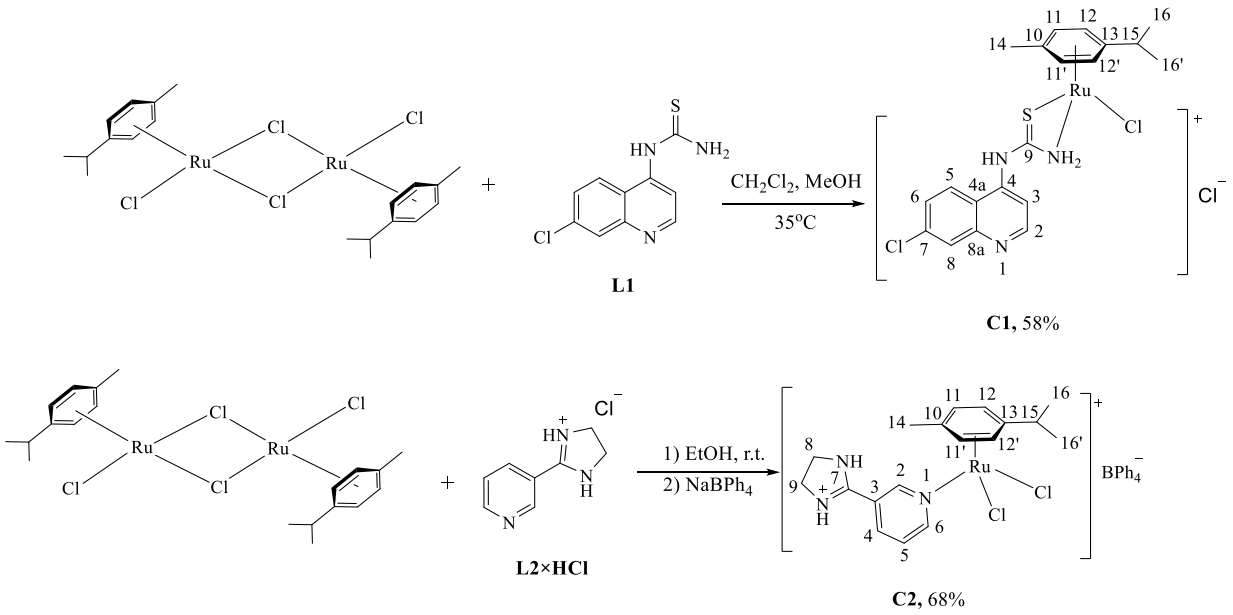

Scheme 2 Synthetic route to complexes [(η^6-*p*-cymene)Ru(L1)Cl]Cl **(C1)** and [(η^6-*p*-cymene)Ru(HL2)Cl_2]BPh_4 **(C2)** and NMR numbering scheme.

Spectral analysis. The IR spectrum of the ligand **L1** exhibited a very strong band around 1600 cm^{-1} and a sharp band around 3200 cm^{-1} due to the C-N and N-H stretching, respectively. The medium band around 1268 cm^{-1} originates from C=S vibration. Additional weak band is observed at around 700 cm^{-1} due to *v*(CS) in free ligand that lacks in spectrum of complex **C1**. The position of C=S band in spectrum of complex **C1** is split in two bands around 1238 cm^{-1} and 1208 cm^{-1}. This strongly suggests that the ligand is bound to the ruthenium center via the sulfur atom from thiourea group.[30] In complex **C2** a strong band at 1600 cm^{-1} from pyridine *v*(C=N) of the complex shows a downward shift of up to 10 cm^{-1} relative to the multiple bands observed in the free ligand. The electronic absorption spectra of complexes **C1** and **C2** were recorded in acetonitrile in the range of 800 – 200 nm. Based on the position and nature of the peaks, all the bands are assigned to either intraligand n $\rightarrow$ π^* and $\pi \rightarrow \pi^*$ transitions or MLCT and LMCT. The mass spectra of complexes show fragmentation patterns that prove the coordination of

ligands. The ESI mass spectra of complexes **C1** and **C2** were recorded in the positive mode. For complex **C1** signal at *m/*z 472.0189 appears when complex cation $[(\eta^6\text{-}p\text{-cymene})Ru(L1)Cl]^+$ loses hydrochloric acid to form $[(\eta^6\text{-}p\text{-cymene})Ru(L1–H)]^+$ cation (Figure S1). For complex **C2** signal at 382.0903 *m/z* appears when complex cation $[(\eta^6\text{-}p\text{-cymene})Ru(HL2)Cl_2]^+$ loses 2 molecules of hydrochloric acid to form $[(\eta^6\text{-}p\text{-cymene})Ru(L2–H)]^+$ cation (Figure S2).

In the ^1H and $^{13}C\{^1H\}$ NMR spectra of both complexes characteristic signals from coordinated *p*-cymene appear at expected shifts.

*Complex **C1***. Values of corresponding integrals for signals **L1** and *p*-cymene reveal their presence in 1:1 molar ratio. In the complex **C1**, all protons from ligand **L1** are shifted when compared with the free ligand, which thus confirmed coordination of **L1** to central ion. Protons from $S=CNH_2$ moiety within thiourea group at 8.33 and 7.75-7.60 ppm (inseparable multiplet with H6) in free **L1** were shifted down-field and appeared at 8.59 and 8.16 ppm. Protons H3 and H5 at 8.10 and 8.11 ppm respectively, both appeared as doublets in free **L1** were shifted down-field, and appeared as multiplet at 8.37-8.32 ppm (inseparable multiplet) in **C1**. Remaining protons from quinoline ring were also slightly shifted down-field. Comparison of $^{13}C\{^1H\}$ NMR spectra of free ligand **L1** and complex **C1** showed that all carbon atoms, with exception of C9, changed their chemical shifts. Thiocarbonyl carbon retained position at 182 ppm. Following carbons were shifted mostly (free **L1** *vs*. **C1** ppm): C4 (143.24 *vs*. 145.96), C8a (149.13 *vs*. 145.96), C8 (127.80 *vs*. 125.21) overlapped with C5 (124.74 *vs.* 125.21), C2 (151.79 *vs*. 149.38), C3 (115.69 *vs.* 113.31). Based on the NMR data we can suggest that ligand **L1** was coordinated through thioamide group to central ion. Strong support for this assumption was obtained from $^1H\text{-}^{15}N$ HSQC NMR spectra for $S=C\text{-}NH_2$ moiety of ligand **L1** and complex **C1.** $^1H\text{-}^{15}N$ HSQC NMR spectrum revealed cross peaks at 131.02/9.22 and 131.02/9.05 ppm for free **L1**, and

122.34/8.67 and 122.34/8.57-8.47 ppm for complex **C1**, which were assigned to ^{15}N-^{1}H coupling within S=C-NH_2.[31] Observed up-field shift of 8.68 ppm for ^{15}N strongly indicate coordination of ligand **L1** to central ion through thioamide group. Corresponding ^{1}H, $^{13}C\{^{1}H\}$ and ^{1}H-^{15}N HSQC NMR spectra for **L1** and **C1** are given in Supporting information (Figures S3 – S10).

*Complex **C2***. Values of corresponding integrals for signals belonging to BPh_4^-, **L2×HCl** and *p*-cymene reveal that they are present in 1:1:1 molar ratio. All signals of pyridine protons in complex **C2** are shifted up-field in comparison with corresponding signals in uncoordinated ligand and thus confirmed coordination to central ion. The most significant changes could be observed for protons H4 at 8.29 ppm, H2 at 9.09 ppm in comparison with the corresponding protons in **L2×HCl** - 8.74 and 9.39 ppm, respectively. Protons H5 and H6 were less shifted, and protons H8 and H9 did not change their positions. Signals belonging to carbons in pyridine ring changed their positions, and the following carbons were shifted the most (free **L2×HCl** *vs*. **C2** ppm): C4 (138.47 *vs.* 136.41), C6 (153.31 *vs.* 155.04), C7 (162.88 *vs.* 163.90) and C2 (148.39 *vs.* 149.19). Signals belonging to C8 and C9 from imidazolidine moiety did not change their position significantly. ^{1}H-^{15}N HMBC NMR spectra of ligand **L2** revealed cross peaks at 316.7/9.29 and 316.7/8.77 ppm assigned to ^{15}N-^{1}H couplings of pyridine nitrogen with H2 and H6. Additional cross peaks were observed at 251/3.85 and 127.73/3.85 ppm that were assigned to ^{15}N-^{1}H couplings of imidazoline nitrogens with H8 and H9.[32] ^{1}H-^{15}N HMBC NMR spectra of complex **C2** revealed cross peaks at 317.65/9.08 and 317.65/8.9 ppm that were assigned to ^{15}N-^{1}H couplings of pyridine nitrogen with H2 and H6. An additional cross peak, although weak, was observed at 115.33/4.0 and it was assigned to ^{15}N-^{1}H couplings of imidazoline nitrogens with H8 and H9. During ^{1}H-^{15}N HMBC experiments **L2** were recorded as base, and for that reason only changes for pyridine nitrogen should be considered. A small down-filed shift for pyridine

nitrogen was observed, which could suggest influence of coordination of **L2** to central ion. Based on the above analysis we suggest that ligand **L2×HCl** is coordinated as cation through nitrogen atom in pyridine ring to central ion. Corresponding ^{1}H, ^{13}C{^{1}H} and ^{1}H-^{15}N HMBC NMR spectra for **L2×HCl** and **C2** are given in Supporting information (Figures S11 – S18).

Stability of complexes C1 and C2. In addition to the general application in structure solving, NMR spectroscopy has been widely used for the thermodynamic and kinetic studies.[33] We used NMR spectra for evaluation of stability of synthesized complexes. Within this research, we planned to examine biological activity of complexes **C1** and **C2**, and according to applied assay (vide infra) complexes should have high stability in DMSO. Since both **C1** and **C2** are very well soluble in same solvent, DMSO-d_6 was chosen for stability studies. Spectra were recorded at room temperature at regular intervals during 24 hours. ^{1}H NMR spectra showed no changes during that time. Position of characteristic signals belonging to the ligands and *p*-cymene did not change their positions, and relative ratios of integrals of corresponding signals remained the unchanged (Figures S19 - S24). Comparison of ^{1}H NMR spectra of complexes **C1** and **C2** with corresponding spectra of the free ligands **L1** and **L2**, and with complex [Ru(cymene)Cl_2DMSO] showed that no substitutions of ligands with DMSO molecules, or any other changes in structures occurred, thus the complexes could be considered as stable. Furthermore, results suggested that complexes would be stable in the applied bioassays.

Conductivity measurements. In order to obtain additional informations about structures of the complexes the conductivity of their solutions was measured. Since complexes exhibited good solubility in different solvents we used methanol and DMSO as solvents for **C1**, and acetonitrile for **C2**. Conductivity values for 1mM solutions of **C1** in DMSO and methanol are

16.21$\Omega^{-1}cm^2mol^{-1}$ and 80 $\Omega^{-1}cm^2mol^{-1}$, respectively, while the conductivity value for **C2** in acetonitrile is 114.5 $\Omega^{-1}cm^2mol^{-1}$. Conductivity of solution depends on the electrolyte type, but it depends on the solvent as well. From the observed conductivities, and based on the literature data[34], we concluded that both complexes are 1:1 type of electrolytes.

Based on the spectral analysis, stability and conductivity measurements we propose the following structures for complexes **C1** and **C2** (Figure 1): in complex **C1** ligand **L1** is coordinated as bidentate through thioamide group, occupying two coordination sites. In complex **C2** ligand **L2** is coordinated as a monodentate cation, through pyridine nitrogen. The coordination spheres are completed with *p*-cymene and one chloride anion (**C1**) or two chloride anions (**C2**).

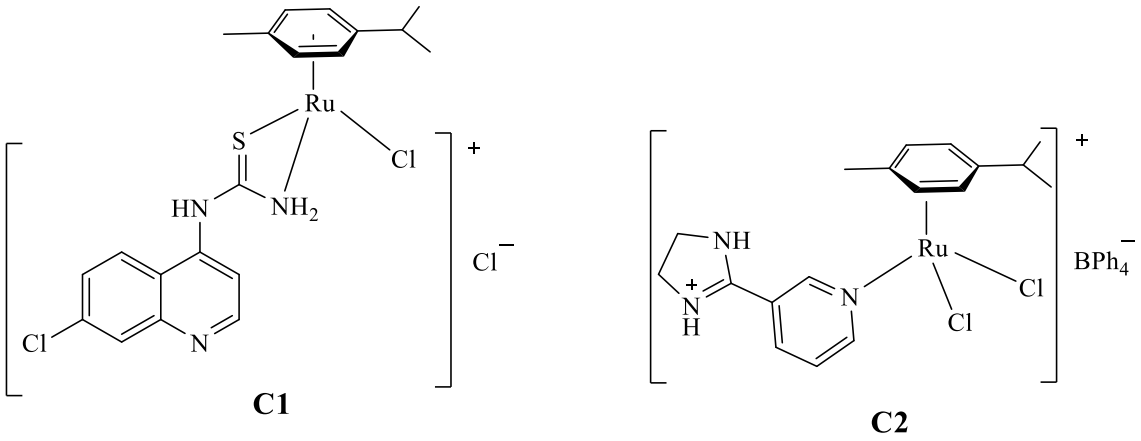

Figure 1. Proposed structures of complexes **C1** and **C2**.

MTT assay. The cytotoxic activities of ruthenium(II) complexes **C1**, **C2**, corresponding ligands **L1**, **L2×HCl**, and *cis*-diamminedichloridoplatinum(II) (cisplatin, **CDDP**) as a referent compound, were evaluated for 72 hours of continuous drug action, by using colorimetric MTT assay. Study was performed in five human neoplastic cell lines (HeLa, K562, A549, MDA-MB-

231, EA.hy 926) and in one non-tumor human fetal lung fibroblast cell line (MRC-5), which was used as non-cancerous model for *in vitro* toxicity evaluation. The obtained results presented as IC_{50} values (Table 1) showed that the tested complexes exhibited cytotoxicity towards all tested cell lines, with IC_{50} values in the range 11.03 - 56.45 μM. Ligands **L1** and **L2×HCl** did not show cytotoxic activity (IC_{50}) up to 100 μM and could be considered as inactive against tested cell lines. Results clearly demonstrated substantial contribution of coordination of ligands **L1** and **L2×HCl** to the cytotoxic activity of the tested complexes. Complex **C1** exhibited better cytotoxicity when compared with **C2**, with the exception towards the HeLa cells. Against that cell line **C2** is approximately two-fold more active than **C1**. The lowest IC_{50} values (μM) for **C1** were observed in human erythromyeloblastoid leukemia cells (K562) (Figure 2a), and human transformed endothelial cells (EA.hy 926) (Figure 2b): 11.03 ± 1.39 and 13.8 ± 2.51 respectively, which were close to the IC_{50} values of **CDDP** (10.86 ± 0.55 and 7.79 ± 1.2 respectively). MTT assay in MRC-5 cells, revealed decreased toxicity of both **C1** and **C2** in comparison to CDDP. Particularly **C1** showed approximately three-times less cytotoxicity in MRC-5 cells (Figure 2c), than in tumor K562 and EA.hy 926 cells, which suggested its cytoselective potential towards the tumor cells. Ability of ruthenium complexes with different structures to exhibit moderate cytotoxicity *in vitro* against the non-tumor cell models, while being selectively cytotoxic towards particular cancer cell lines, often lymphoid, has already been reported.[35] Structure-activity comparison in the present study clearly revealed that higher cytotoxicity and cytoselectivity towards tumor cells of **C1** in comparison to **C2** is contribution of coordinated ligand **L1**. Graphics with cell survival after 72 hours treatment of A549, HeLa and MDA-MB-231 cell lines with ligands **L1**, **L2**, complexes **C1**, **C2** and **CDDP** are given in Supporting Information (Figures S25 – S27).

Table 1. *In vitro* cytotoxicity of compounds **C1**, **C2**, **L1**, **L2×HCl** and **CDDP** against human cell lines after 72 hours of continuous drug action.

Cell line[a]	**Compound**				
IC_{50} (μM)	**C1**	**C2**	**L1**	**L2×HCl**	**CDDP**[i]
HeLa[b]	56.45±1.59	28.62±1.72	>100[h]	>100	7.59±0.04
K562[c]	11.03±1.39	54.86±6.6	>100	>100	10.86±0.55
MDA-MB-231[d]	26.62±7.24	47.66±1.02	>100	>100	13.24±0.4
EA.hy 926[e]	13.8±2.51	25.34±3.57	>100	>100	7.79±1.2
A549[f]	31.49±5.63	39.77±0.79	>100	>100	17.2±0.7
MRC-5[g]	33.7±5.47	42.54±6.7	>100	>100	11.54±0.5

[a] IC_{50} values (μM) are presented as and average ± SD from three or more independent experiments. [b]HeLa: human cervix cancer cell line; [c] K562: human myelogenous leukemia cell line; [d] MDA-MB.231: human breast cell line; [e] EA.hy 926: human endothelial cell line; [f] A549 human lung adenocarcinoma epithelial cell line; [g] MRC-5: non-tumor human lung fibroblast cells; [h] > 100 denotes that IC_{50} was not obtained in the range of concentrations tested up to 100 μM.[i] **CDDP** = *cis*-diamminedichloridoplatinum(II) (cisplatin).

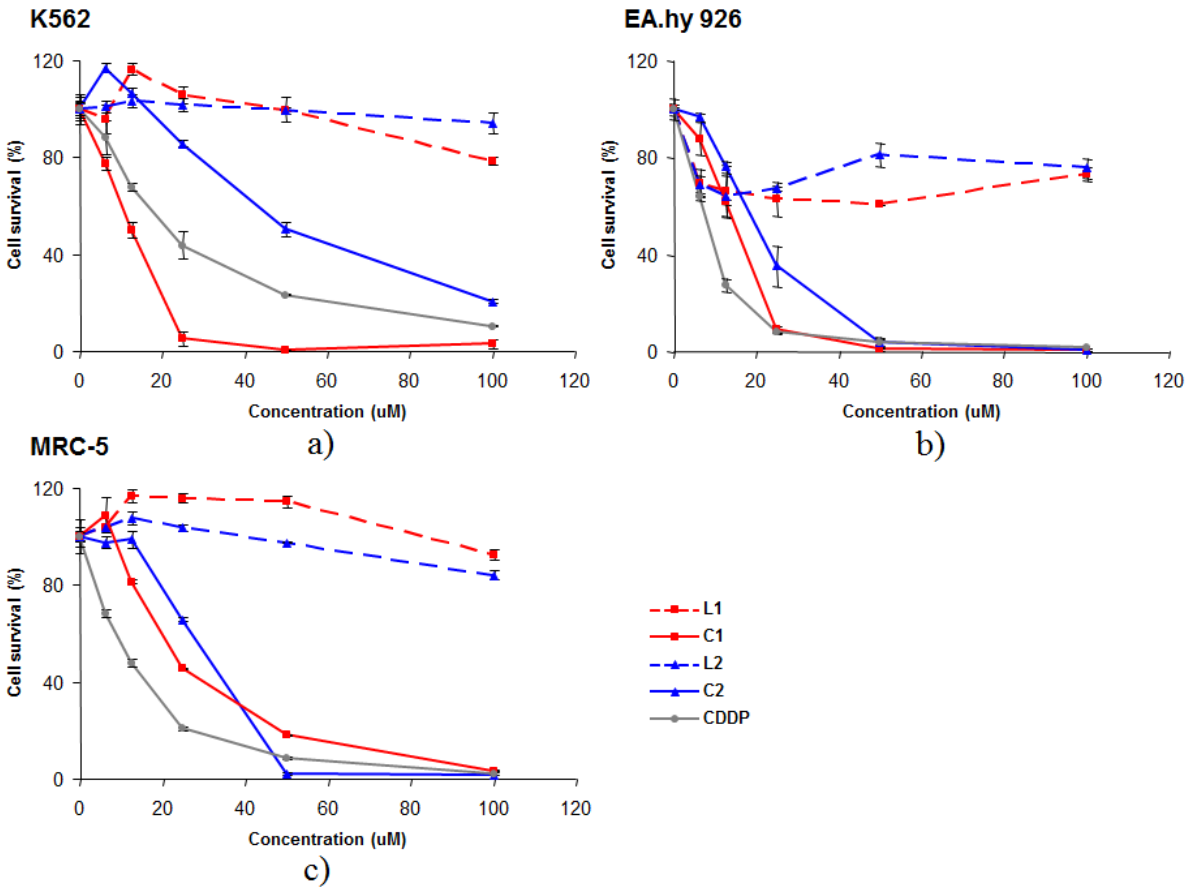

Figure 2. Cell survival after 72 hours treatment with ligands **L1**, **L2,** complexes **C1**, **C2** and **CDDP** of: a) K562 cell line, b) Ea.hy 926 cell line, c) MRC-5 cell line.

Cell cycle analysis by flow cytometry. In order to investigate whether the tested ruthenium complexes inhibited cancer cell growth through suppression of cell cycle, flow cytometry analysis of the cell cycle phase distribution was examined in K562 cells, by using staining with propidiumiodide (PI). K562 cells were chosen for further analysis due to their high sensitivity to the action of **C1**, in the level comparable to that of cisplatin. The effect of the tested agents or cisplatin was analyzed at two different concentrations (IC_{50} and $2\times IC_{50}$). At the lower concentration, the tested agents did not significantly alter the cell cycle progression. At $2\times IC_{50}$, cisplatin caused loss of DNA at G2-M and a subsequent increase of sub-G1 content. **C1** and **C2**

also induced concentration dependent accumulation of cells in sub-G1 fraction (Figure 3, Table 2), in the extent similar to cisplatin. Generation of sub-G1 peak is considered as a hallmark of internucleosomal DNA cleavage, as the result of apoptotic cell death.[36,37] However **C1** and **C2** did not cause any other alterations of the cell cycle, following the 24 hours action. This result may not be unexpected, since the ability of some Ru-arene complexes, to generate cytotoxic effect with just moderate or no effect on cell cycle, was reported previously.[38,39]

Free ligand did not induce changes in the sub-G1 fraction, relative to control, which is consistent with its lack of cytotoxicity. Minor arrest in the S phase was caused by **L1**, and seemed to be concentration independent (approximately 29.3% at both IC_{50} and $2\times IC_{50}$, compared with the control 21.3%). Slight S phase delay, might indicate interference of 7-chloroquinolineligand with cellular DNA.[40] Earlier studies on quinoline-based antibacterial agents (such as Ciprofloxacin), have demonstrated the potential of quinoline derivatives to inhibit topoisomerase in HeLa cells, and DNA-gyrase in bacteria, at higher concentrations, while Ciprofloxacin-treated K562 cells progressed more slowly through the S and G2/M stages of the cell cycle.[41]

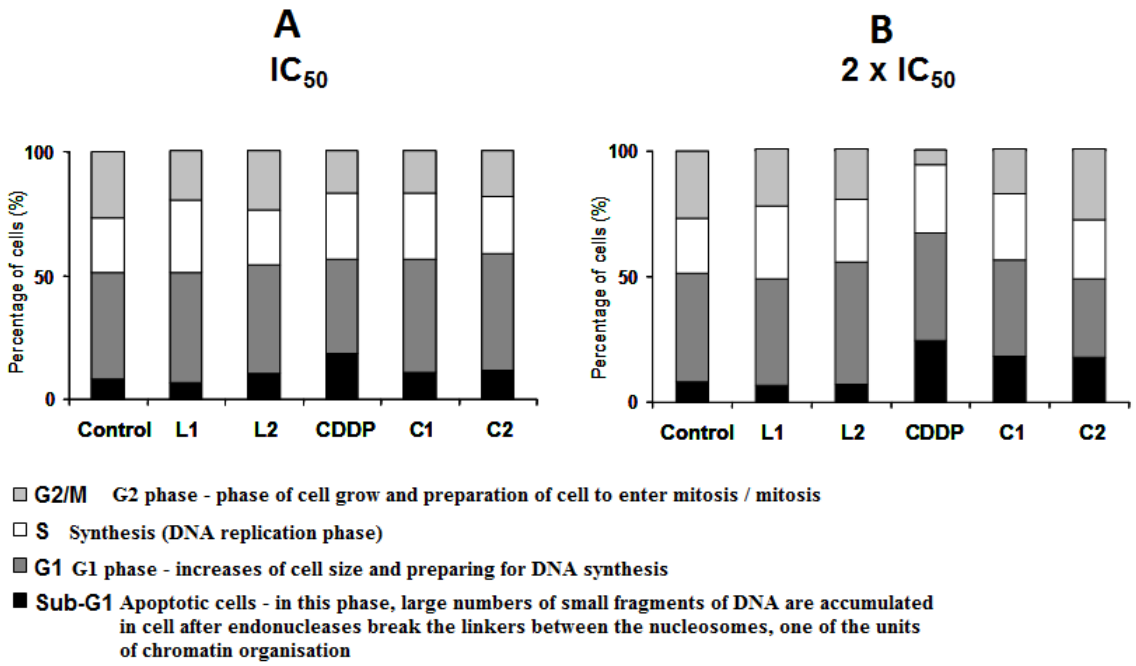

Figure 3. Diagrams of cell cycle phase distribution of treated K562 cells after 24 hours treatment with **L1**, **L2**, **CDDP, C1** and **C2** at concentration corresponding to (A) IC_{50} and (B) $2{\times}IC_{50}$.

Table 2. Percentage of cells in sub-G1 fraction of cell cycle, after 24 hours treatment with **L1**, **L2**, **CDDP, C1** and **C2** at concentration corresponding to IC_{50} and $2{\times}IC_{50}$.

	Sub G1 fraction (%)	
	IC_{50}	**$2{\times}IC_{50}$**
Control	8.06 ± 0.00	8.1 ± 0.00
L1	6.57 ± 0.0.02	6.5 ± 0.57
L2	10.38 ± 0.41	6.9 ± 0.08

CDDP	18.47 ± 1.38	24.4 ± 1.38
C1	10.84 ± 0.71	18.4 ± 0.33
C2	11.84 ± 0.00	17.9 ± 1.5

Gasser et al. reported that ruthenium complexes [Ru(η^6-arene)(L)Cl_2], similar to **C1** and **C2**, where L is N-heterocyclic ligand: pyridine, imidazoles, quinoline and their derivatives, undergo solvolysis by DMSO and release of ligands.[42] Ligand-exchange reaction on ruthenium ion caused by DMSO, tends to reach an equilibrium, in which, according to Turel, 10–50% of ligand may remain free.[12] However, in the aqueous solutions, exchange of the anionic (halogenide) ligands is considered to be a part of complex activation. The newly formed complex has enhanced reactivity with nucleophilic targets in the cells.[43] Complex chemical behavior of ruthenium(II)-arene complexes, raises a question of whether the prominent cytotoxicity of **C1** and **C2** may resulted from the similar process which includes solvolysis of one or more ligands from the initial complexes, and also that pertaining to the structure of active complex, which may bind to DNA or inhibit transcription processes.[44] We found that there were no changes in the structures of complexes **C1** and **C2** in DMSO solution during 24 hours. In ^{1}H NMR chemical shifts of the coordinated ligands remained at same position and no changes of ratios of integrals of the corresponding signals were detected (see Figures S19 - S24). Based on the obtained activities of the complexes **C1** and **C2**, and corresponding ligands **L1** and **L2×HCl**, and the observed stability of the tested complexes it could be concluded that the active complexes have the structures proposed in Figure 1. An additional study is needed to elucidate faith of the initial complex **C1** in biological medium and to investigate feasible mechanism of action.

ICP-MS measurement of intracellular ruthenium(II) accumulation. In order to determine the level of intracellular accumulation of the novel ruthenium(II) complexes **C1** and **C2**, versus accumulation of **CDDP**, ICP-MS study was performed in K562 cells, following the 24 hours treatment with equal concentrations (50 μM) of compounds (Figure 4A). The obtained results are presented as plot of metal concentration Ru(II) or Pt(II), recorded inside the cells, normalized upon the cell number (μg/10^6 cells). The obtained data indicated that **C1** entered cells more efficiently compared with **CDDP**. Intracellular ruthenium concentration (**C1**): 1.38±0.166 (μgRu/10^6 cells) exceeded that of **CDDP**: 0.299±0.002 (μgPt/10^6 cells) by approximately 4.6 times. Complex **C2** exhibited poor intracellular accumulation, 0.081±0.004 (μgM/10^6 cells) at same concentration, which was in accordance to its lower activity. Ruthenium-arene complexes of similar structures containing quinoline derivatives, were initially synthesized as successful antibacterial and antimalarial agents, and were characterized by good transport behavior and balanced structural and lipophilic properties.[41,45] A number of studies highlighted the relevance of lipophilicity on drug influx and activity, and there is a clear correlation between drug intracellular accumulation and cytotoxicity in numerous cell lines.[46] Accordingly, the obtained data in the present study demonstrated significantly higher intracellular accumulation of **C1** versus **C2** and **CDDP**, and clearly indicated positive effect of the quinoline moiety on cellular uptake of Ru(η^6-*p*-cymene) complexes.

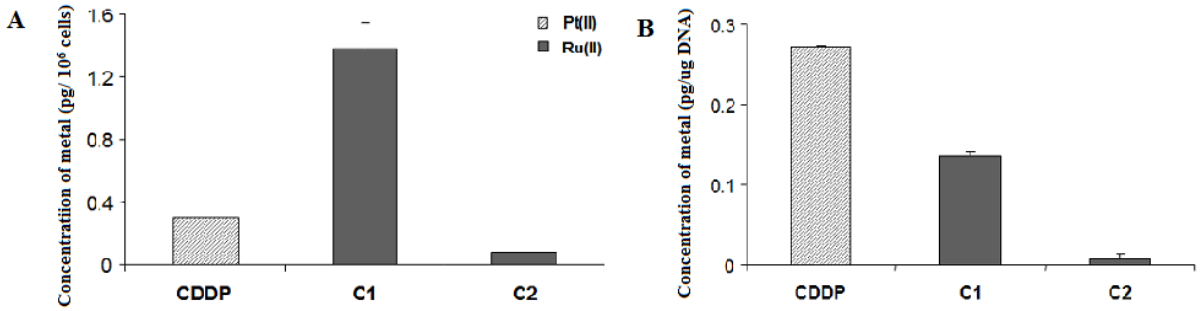

Figure 4. Concentrations of platinum(II)/ruthenium(II) after 24 hours treatment of K562 cells with equimolar concentrations (50 μM) of **C1**, **C2** or **CDDP**: A) intracellular concentrations (μg/10^6cells), B) concentrations (pg/μg) bounded to cellular-DNA. Bar graphs represent mean values of three independent measurements.

ICP-MS measurement of ruthenium(II)-DNA binding. Cellular DNA is a common target of cytotoxic action of metal-based complexes. Ru(II) compounds might interact with DNA directly, inducing conformational changes, crosslinks or strand breaks,[47,48] or may damage DNA indirectly through induction of mitochondrial-apoptotic cell death or oxidative stress.[47,49] In order to assess capability of the complexes **C1** and **C2** to bind DNA in K562 cells, the ICP-MS study was performed following 24 hours treatment. Cells were collected immediately after the treatment and nuclear DNA was isolated and quantified. Stock solutions of DNA gave a ratio of UV absorbance A260/A280 of 2.3-2.8, indicating that the DNA was sufficiently free of protein contamination. The results of ICP-MS study (Figure 4B), showed that both ruthenium complexes binds to cellular DNA less efficiently when compared with **CDDP**. The level of DNA platination, 0.271 ± 0.001 pg Pt/ug DNA, was two times higher than the level of DNA-ruthenium binding caused by **C1**: 0.135 ± 0.005 pg Ru/μg DNA. Poor DNA binding of **C2**: 0.007± 0.006 pg Ru/μg DNA, was in accordance to its lower intracellular accumulation and the generally lower

cytotoxicity. The ratio of DNA binding (relative to the amount of complex present in the cell) decreased in order: **CDDP** > **C1** > **C2**. Although **C1** exhibited comparable *in vitro* activity to **CDDP** in K562, our conclusion is that its mechanism of cytotoxic action could not be explained only by the DNA binding capability, or at least that DNA might not be the only intracellular target, for this type of complexes.

Reduced DNA binding of **C1** compared with cisplatin, may be due to the additional interactions with proteins or peptides carrying sulfur donor groups, such as cysteine, methionine, glutathione (GSH), which are known to intercept metal-drugs prior the entrance into the nucleus and which have an important role in the mechanisms of metal-drugs toxicity and resistance.[50,51] The exact mechanism of action of ruthenium-based complexes is still largely unknown. Though **C1** bind to DNA, it might induce different DNA conformational changes than cisplatin, due to the different complex geometry, and in addition, it may interact to the non-nuclear targets, such as the mitochondrion or the cellular enzymes.[52] A promising possibility for cell-specific activation of metal-based drugs may be through ligand-stereoselective catalysis, mediated by certain cellular enzymes, which are often found in highly increased concentrations in tumor tissue.[53] Altogether, results obtained in the present study are in agreement to the previously referred literature of ruthenium complexes with *p*-cymene as arene, which have shown cytotoxicity comparable to that of cisplatin in a number of cell lines[35c,50,54] though nuclear DNA might not represent the single target in the mechanism of cytotoxicity of these compounds.

CONCLUSION

In this work one new ligand and two new ruthenium-*p*-cymene complexes have been prepared. Based on spectroscopic data, usual piano-stool geometry of complexes was proposed.

According to our *in vitro* biological studies on the panel of five cell lines, **C1,** contained 7-chloroquinoline-4-thiourea ligand, displayed the prominent action in human erythromyeloblastoid leukemia cells (K562), comparable to that of cisplatin, while being cytoselective and three times less toxic in non-tumor MRC-5 cells. Complexes **C1** and **C2,** at the applied cytotoxic concentrations ($2\times IC_{50}$), exhibited similar capability to induce apoptotic sub-G1 fraction, in the absence of other substantial alterations of cell cycle. Results obtained with the ICP-MS study revealed differences in the affinity for cellular uptake and DNA binding of tested complexes. Intracellular uptake of **C1** exceeded that of **CDDP** and **C2**, by approximately 4.6 and 10-times, respectively, while the level of DNA binding (pg of metal/μg DNA) decreased in following order **CDDP** > **C1** > **C2** implicating, that cellular DNA, might not present the only target of cytotoxic action of this type of complexes. Certainly, additional study is needed in order to address mechanism of action and selectivity of **C1** toward K562 cells. Structure-activity comparison suggested that introduction of 7-chloroquinoline-4-thiourea moiety to ruthenium(II)-*p*-cymene, markedly enhanced intracellular uptake of **C1** and contributed to the cell-specific cytotoxicity. Reduced drug accumulation is one of the major limitations to the successful chemotherapy treatment and is among the major factors responsible for the development of tumor cell resistance. Present study demonstrated that introduction of 7-chloroquinoline-4-thiourea ligand to the ruthenium arene of general structure $[Ru(\eta^6\text{-arene})(L)Cl_2]$ may provide a way to the design of complexes with an encouraging cellular-uptake properties.

ASSOCIATED CONTENT

Supporting Information

The Supporting Information includes mass spectra of complexes, NMR spectra of ligands and complexes, additional graphics of cell survival after treatment of A549, HeLa and MDA-MB-231 cell lines with compounds **L1**, **L2×HCl**, **C1**, **C2** and **CDDP**. This material is available free of charge via the Internet at http://pubs.acs.org.

AUTHOR INFORMATION

Corresponding Authors

* For D.M.O.: phone +381-11-333-66-81; fax, +381-11-263-60-61; E-mail: dopsen@chem.bg.ac.rs.

* For S.G.-Š.: phone +381-11-333-67-42; fax, +381-11-218-43-30; E-mail: sanjag@chem.bg.ac.rs.

Author Contributions

The manuscript was prepared through contributions of all authors. All authors have given approval to the final version of the manuscript.

NOTE

The authors declare no competing financial interest

ACKNOWLEDGEMENTS

This work was supported by the Ministry of Education, Science and Technological Development of the Republic of Serbia, grant numbers 172035, 172008 and III 41026. The authors acknowledge the support of the FP7 RegPot project FCUB ERA GA No. 256716. The EC does

not share responsibility for the content of the article. We thank COST Action CM1105 for stimulating discussions.

REFERENCES

(1) (a) Gasser, G.; Metzler-Nolte, N. *Curr. Opin. Chem. Biol*. **2012**, *16*, 84–91. (b) Noffke, A.L.; Habtemariam, A.; Pizarro, A. M.; Sadler, P. J. *Chem. Commun*. **2012**, *48*, 5219-5246. (c) Süss-Fink, G. *Dalton Trans*. **2010**, *39*, 1673-1688; d) Barry, N. P. E.; Sadler, P. J. *Chem. Commun*. **2013**, *49*, 5106–5131.

(2) Pettinari, R.; Pettinari, C.; Marchetti, F.; Clavel, C. M.; Scopelliti, R.; Dyson, P. J. *Organometallics* **2013**, *32*, 309-316.

(3) Bratsos, I.; Mitri, E.; Ravalico, F.; Zangrando, E.; Gianferrara, T.; Bergamo, A.; Alessio, E. *Dalton Trans.* **2012**, *41*, 7358-7371.

(4) (a) Ang, W. H.; Casini, A.; Sava, G.; Dyson, P. J. *J. Organomet. Chem.* **2011**, *696*, 989–998. (b) Liu, H.- K.; Sadler, P. J. *Acc. Chem. Res.* **2011**, *44*, 349–359. (c) Kandioller, W.; Balsano, E.; Meier, S. M.; Jungwirth, U.; Göschl, S.; Roller, A.; Jakupec, M. A.; Berger, W.; Keppler B. K; Hartinger, C. G. *Chem. Commun*. **2013**, *49*, 3348-3350. (d) Gasser, G.; Ott, I.; Metzler-Nolte, N. *J. Med. Chem.* **2011**, *54*, 3–25. (e) Hartinger, C. G.; Metzler-Nolte, N.; Dyson, P. J. *Organometallics* **2012**, *31*, 5677–5685. (f) Smith G. S.; Therrien, B. *Dalton Trans.* **2011**, *40*, 10793–10800.

(5) Hillard, E. A.; Vesseires, A.; Jaouen, G. *Top. Organomet. Chem.* **2010**, 32, 81-117.

(6) Biot, C.; Daher, W.; Chavain, N.; Fandeur, T.; Khalife, J.; Dive, D.; De Clercq, E. *J. Med. Chem.* **2006**, *49*, 2845-2849.

(7) Liu, H.; Yang, H.; Xu, J.; Wang, J.; Nie, R.; Li, C. *Malaria J.* **2013**, *12*, 409/1-409/7.

(8) Ganguly, S.; Saha, P.; Guha, S. K.; Das, S.; Bera, D. K.; Biswas, A.; Kundu, P. K.; Saha, B.; Ray, K.; Majia, A. K. *Antimicrob. Agents Ch.* **2013**, *57*, 1246-1251.

(9) Glans, L.; Ehnbom, A.; de Kock, C.; Martínez, A.; Estrada, J.; Smith, P. J.; Haukka, M.; Sánchez-Delgado, R. A.; Nordlander, E. *Dalton Trans*. **2012**, *41*, 2764-2773.

(10) Rajapakse, C. S. K.; Martínez, A.; Naoulou, B.; Jarzecki, A.; Suárez, L.; Deregnaucourt, C.; Sinou, V.; Schrével, J.; Musi, E.; Ambrosini, G.; Schwartz, G. K.; Sánchez-Delgado, R. A. *Inorg. Chem.* **2009**, *48*, 1122-1131.

(11) Gobec, M.; Kljun, J.; Sosič, I.; Mlinarič-Raščan, I.; Uršič, M.; Gobec, S.; Turel, I. *Dalton Trans.* **2014**, *43*, 9045-9051.

(12) Kljun, J.; Bratsos, I.; Alessio, E.; Psomas, G.; Repnik, U.; Butinar, M.; Turk, B.; Turel, I. *Inorg. Chem.* **2013**, *52*, 9039-9052.

(13) Kljun, J.; Bytzek, A. K.; Kandioller, W.; Bartel, C.; Jakupec, M. A.; Hartinger, C. G.; Keppler, B. K.; Turel, I. *Organometallics* **2011**, *30*, 2506-2512.

(14) Egan, T. J.; Marques, H. M., *Coordin. Chem. Rev.*, **1999**, *190–192*, 493–517.

(15) Cheng, J.; Zeidan, R.; Mishra, S.; Liu, A.; Pun, S. H.; Kulkarni, R. P.; Jensen, G. S.; Bellocq, N. C.; Davis, M. E.; *J. Med. Chem.* **2006,** *49*, 6522-6531.

(16) Anastassiadou, M.; Danoun, S.; Crane, L.; Baziard-Mouysset, G.; Payard, M.; Caignard, D.-H.; Rettori, M.-C.; Renard, P. *Bioorgan. Med. Chem.* **2001**, *9*, 585-592.

(17) Barr, M. P.; Gray, S. G.; Hoffmann, A. C.; Hilger, R. A.; Thomale, J.; O'Flaherty, J. D.; Fennell, D. A.; Richard, D.; O'Leary, J. J.; O'Byrne, K. J., *PLoS One.*, **2013**,*8*: e54193. doi:10.1371/journal.pone.0054193.

(18) Jensen, S. B.; Rodger, S. J.; Spicer, M. D. *J. Organomet. Chem.* **1998**, *556*, 151-158.

(19) (a) Bhat, H. R.; Singh, U. P.; Gahtori, P.; Ghosh, S. K.; Gogoi, K.; Prakashd, A.; Singh, R. K. *RSC Adv.* **2013**, *3*, 2942–2952; (b) Zhong, B.; Al-Awar, R. S.; Shih, C.; Grimes, J. H. Jr.; Vieth, M.; Hamdouchi, C. *Tetrahedron Lett.* **2006**, *47*, 2161–2164.

(20) Although these results are outside the range viewed as establishing analytical purity, they are provided to illustrate the best values obtained to date.

(21) Supino, R. *Methods Mol. Biol*. **1995**, *43*, 137-149.

(22) Ivanović, I.; Gligorijević, N.; Aranđelović, S.; Radulović, S.; Roller, A.; Keppler, B. K.; Tešić, Ž. Lj.; Grgurić-Šipka, S.; *Polyhedron* **2013**, *61*, 112–118.

(23) Ormerod, M. G. Analysis of DNA-general methods, in: M.G. Ormerod (Ed.), Flow Cytometry, a Practical Approach, Oxford University Press, New York **1994**, 119-125.

(24) Gehrke, H.; Pelka, J.; Hartinger, C. G.; Blank, H.; Bleimund, F.; Schneider, R.; Gerthsen, D.; Bräse, S.; Crone, M.; Türk, M.; Marko, D. *Arch. Toxicol*. **2011**, *85*, 799–812.

(25) Miller, S. A.; Dykes, D. D.; Polesky, H. F. *Nucleic. Acids. Res*. **1988** *16*, 1215.

(26) Malisić, E.; Janković, R.; Jakovljević, K. *Arch. Gynecol. Obstet.* **2012**, *286*, 723-728.

(27) (a) An, S.; Yin, B.; Liu, P.; Li, X.; Li, C.; Li, J.; Shi, Z. *Synthesis* **2013**, *45*, 2525-2532; (b) Zhang, J.; Wang, X.; Yang, M.; Wan, K.; Yin, B.; Wang, Y.; Li, J. Z. *Tetrahedron Lett.* **2011**, *52*, 1578–1582; (c) Hojati, S. F.; Mohammadpoor-Baltork, I.; Maleki, B.; Gholizadeh, M.; Shafiezadeh, F. *Can. J. Chem.* **2010**, *88*, 135-141; (d) Mohammadpoor-Baltork, I.; Mirkhani, V.; Moghadam, M.; Tangestaninejad, S.; Zolfigol, M. A.; Abdollahi-Alibeik, M.; Khosropour, A. R.; Kargar, H.; Hojati, S. F. *Catal. Commun.* **2008**, *9*, 894–901.

(28) (a) Mohammadpoor-Baltork, I.; Moghadam, M.; Tangestaninejad, S.; Mirkhani, V.; Hojati, S. F.; *Polyhedron* **2008**, *27*, 750–758; (b) Sun, M.; Wei, H. T.; Li, D.; Zheng, Y.-G.; Cai, J.; Min Ji, *Synthetic Commun.* **2008**, *38*, 3151–3158; (c) Moghadam, M.; Mohammadpoor-Baltork, I.; Mirkhani, V.; Tangestaninejad, S.; Abdollahi-Alibeik, M.; Yousefi, B. H.; Kargar, H. *Monatsh. Chem.* **2007**, *138*, 579–583; (d) Mirkhani, V.; Mohammadpoor-Baltork, I.; Moghadam, M.; Tangestaninejad, S.; Abdollahi-Alibeik, M.; Kargar, H. *Appl. Catal. A- Gen.* **2007**, *325*, 99–104; (e) Anastassiadou, M.; Danoun, S.; Crane, L.; Baziard/Mouysset, G.; Payard, M.; Caignard, D. -H.; Rettori, M. -C.; Renard, P. *Bioorg. Med. Chem.* **2001**, *9*, 585–592.

(29) Mirkhani, V.; Moghadam, M.; Tangestaninejada, S.; Kargara, H. *Tetrahedron Lett.* **2006**, *47*, 2129–2132.

(30) Sheeba, M. M.; Tamizh, M. M.; Farrugia, L. J.; Endo, A.; Karvembu, R. *Organometallics* **2014**, *33*, 540−550.

(31) Chemical shifts for 1H of S=C-NH2 were obtained from 1H NMR recorded at 500 MHz during 1H-15N HSQC NMR experiment. Corresponding specta are given in Supporting information as Figures S7 and S9.

(32) Chemical shifts for 1H of **L2** and **C2**were obtained from 1H NMR recorded at 500 MHz during 1H-15N HMBC NMR experiment. Corresponding specta are given in Supporting information as Figures S15 and S17.

(33) (a) Gallego, D.; Inoue, S.; Blom, B.; Driess, M. *Organometallics* **2014**, *33*, 6885-6897. (b) Schmidlehner, M.; Pichler, V.; Roller, A.; Jakupec, M. A.; Kandioller, W.; Keppler, B. K. *J. Organomet. Chem.* **2014**, *772-773*, 93-99.

(34) Geary, W. J. *Coord. Chem. Rev.* **1971**, *7*, 81-122.

(35) (a) De Lima, A. P.; Pereira, Fde C.; Vilanova-Costa, C. A.; Mello, F. M.; Ribeiro, Ade S.; Benfica, P. L.; Valadares, M. C.; Pavanin, L. A.; dos Santos, W. B.; Lacerda, Ede P. *Toxicol. in Vitro* **2010**, *24*, 1562–1568. (b) Martínez, A. C.; Rajapakse, S.; Sánchez-Delgado, R. A.; Varela-Ramirez, A.; Lema, C.; Aguilera, R. *J. Inorg. Biochem*. **2010**, *104*, 967-977. (c) Vock, C. A.; Scolaro, C.; Phillips, A. D.; Scopelliti, R.; Sava, G.; Dyson, P. J. *J. Med. Chem*. **2006**, *49*, 5552-5561. (d) Savić, A.; Dulović, M.; Poljarević, J. M.; Misirlić-Denčić, S.; Jovanović, M.; Bogdanović, A.; Trajković, V.; Sabo, T. J.; Grgurić-Šipka, S.; Marković, I. *ChemMedChem*. **2011**, *6*, 1884-1891.

(36) Huang, X.; Halicka, H. D.; Traganos, F.; Tanaka, T.; Kurose, A.; Darzynkiewicz, Z. *Cell Proliferat.* **2005**, *38*, 223-243.

(37) Vock, E. H.; Lutz, W. K.; Hormes, P.; Hoffmann, H. D.; Vamvakasa, S. *Mutat. Res*. **1998**, *413*, 83-94.

(38) Ginzinger, W.; Mühlgassner, G.; Arion, V. B.; Jakupec, M. A.; Roller, A.; Galanski, M.; Reithofer, M.; Berger, W. B.; Keppler, B. K. *J. Med. Chem*. **2012**, *55*, 3398-3413.

(39) Gligorijević, N.; Aranđelović, S.; Filipović, L.; Jakovljević, K.; Janković, R.; Grgurić-Šipka, S.; Ivanović, I.; Radulović, S.; Tešić, Ž. Lj. *J. Inorg. Biochem*. **2012**, *108*, 53-61.

(40) Rescifina, A.; Zagni, C.; Varrica, M. G.; Pistarà, V.; Corsaro, A. *Eur. J. Med. Chem*. **2014**, *74*, 95-115.

(41) Foresgren, A.; Schlossman, S. F.; Tedder, T .F.; *Antimicrob. Agents Ch*. **1987**, *31*, 768-773.

(42) Patra, M.; Joshi, T.; Pierroz, V.; Ingram, K.; Kaiser. M.; Ferrari, S.; Spingler, B.; Keiser, J.; Gasser, G. *Chem. Eur. J*. **2013**, *19*, 14768–14772.

(43) (a) Betanzos-Lara, S.; Novakova, O.; Deeth, R. J.; Pizarro, A. M.; Clarkson, G. J.; Liskova, B.; Brabec, V.; Sadler, P. J.; Habtemariam, A. *J. Biol. Inorg. Chem*. **2012**, *17*, 1033-1051. (b) Bratsos, I.; Simonin, C.; Zangrando, E.; Gianferrara, T.; Bergamo, A.; Alessio. E. *Dalton Trans*. **2011**, *40*, 9533-9543. (c) Wang, F.; Habtemariam, A.; van der Geer, E. P.; Fernández, R.; Melchart, M.; Deeth, R. J.; Aird, R.; Guichard, S.; Fabbiani, F. P.; Lozano-Casal, P.; Oswald, I. D.; Jodrell, D. I.; Parsons, S.; Sadler, P. J. *Proc. Natl. Acad. Sci*. **2005**, *102*, 18269-18274.

(44) Wheate, N. J.; Brodie, C. R.; Collins, J. G.; Kemp, S.; Aldrich-Wright, J. R. *Mini Rev. Med. Chem*. **2007**, *7*, 627-648.

(45) Singh, A. K.; Pandey, D. S.; Xu, Q.; Braunstein, P. *Coord. Chem. Rev*. **2014**, *271*, 31-56.

(46) (a) Cossa, G.; Gatti, L.; Zunino, F.; Perego, P. *Curr. Med .Chem*. **2009,** *16*, 2355-2365. (b) Buß, I.; Kalayda, G. V.; Lindauer, A.; Reithofer, M. R.; Galanski, M.; Keppler, B. K.; Jaehde, U. J. *J. Biol. Inorg. Chem*. **2012**, *17*, 699-708. (c) Buß, I.; Garmann, D.; Galanski, M.; Weber, G.; Kalayda, G. V.; Keppler, B. K.; Jaehde, U. *J. Inorg. Biochem.* **2011**, *105*, 709-717.

(47) Novakova, O.; Kasparkova, J.; Bursova, V.; Hofr, C.; Vojtiskova, M.; Chen, H.; Sadler, P. J.; Brabec. V. *Chem. Biol*. **2005**, *12*, 121-129.

(48) Brabec, V.; Nováková, O. *Drug. Resist. Update* **2006**, *9*, 111-122.

(49) Qian, C.; Wang, J. Q.; Song, C. L.; Wang, L. L.; Ji, L. N.; Chao, H. *Metallomics* **2013**, *5*, 844-854.

(50) Dougan, S. J.; Habtemariam, A.; McHale, S. E.; Parsons, S.; Sadler, P. J. *Proc. Natl. Acad. Sci*. **2008**, *105*, 11628-11633.

(51) (a) Chen, H. H. W.; Kuo, M. T. *Met. Based Drugs* **2010**, http://dx.doi.org/10.1155/2010/430939. (b) Dzamitika, S.; Salerno, M.; Pereira-Maia, E.; Le Moyec, L.; Garnier-Suillerot, A. *J. Bioenerg. Biomembr*. **2006**, *38*, 11-21. (c) Florea, A. M.; Büsselberg, D. *Cancers* **2011**, *3*, 1351-1371.

(52) (a) Bugarcic, T.; Nováková, O.; Halámiková, A.; Zerzánková, L.; Vrána, O.; Kaspárková, J.; Habtemariam, A.; Parsons, S.; Sadler, P. J.; Brabec, V. *J. Med. Chem*. **2008**, *51*, 5310-5319. (b) Filak, L. K.; Mühlgassner, G.; Jakupec, M. A.; Heffeter, P.; Berger, W.; Arion, V. B.; Keppler, B. K. *J. Biol. Inorg. Chem*. **2010**, *15*, 903-918. (c) a) He, L.; Liao, S. Y.; Tan, C. P.; Ye, R. R.; Xu, Y. W,; Zhao, M.; Ji, L. N.; Mao, Z. W. *Chem. Eur. J.* **2013**, *19*, 12152–12160.

(53) Van Zutphen, S.; Reedijk, J. *Coord. Chem. Rev*. **2005**, *249*, 2845–2853.

(54) Scolaro, C.; Chaplin, A. B.; Hartinger, C. G.; Bergamo, A.; Cocchietto, M.; Keppler, B. K.; Sava, G.; Dyson. P. J. *Dalton Trans*. **2007**, *43*, 5065-5072.